A Spherical Co-ordinate Space Parameterisation for Orbit Estimation

Jose Franco, Emmanuel D. Delande
School of Engineering and Physical Sciences
Heriot-Watt University
Edinburgh, UK

Carolin Frueh
School of Aeronautics and Astronautics
Purdue University
West Lafayette, IN, USA

Jeremie Houssineau, Daniel E. Clark
School of Engineering and Physical Sciences
Heriot-Watt University
Edinburgh, UK

***Abstract*—An interesting challenge in orbital estimation problems for space surveillance using optical sensors is that, since both the orbital mechanics and the sensor observation process are non-linear, the standard filtering solutions such as Kalman filters are inapplicable and lead to divergent results. Naïve particle filtering solutions also fail since they require many particles to accurately represent the posterior distribution. However, since the sensor observation noise is modelled as a multivariate Gaussian distribution, it may be expected that the same single-object probability distributions, once projected into the augmented sensor space (a full spherical frame centred on the sensor), assume a simpler form that can be approximated by a multivariate Gaussian distribution. In this paper, a sequential Monte Carlo filter is proposed for the orbital object estimation problem, which exploits the structure of the measurement likelihood probability by introducing a proposal distribution based on a linear Kalman filter update.**

TABLE OF CONTENTS

1. INTRODUCTION

Obtaining an accurate picture of the position and dynamics of Earth-orbiting objects has been a research topic under growing attention lately, partly due to the growing relevance of safeguarding important assets in orbit from collision with debris or other man-made objects. A diverse range of earth- or ground-based sensors is available to survey space and so gain information on where the objects are [1], but careful statistical techniques must be used to minimise errors induced due to sensor inaccuracy and imperfect modelling of object dynamics. Several problems present themselves when attempting to exploit sensor measurements in order to determine the state of space-based objects:

- Sensors are limited in their field of view, and can only survey a fraction of near-Earth space at any given time;
- No sensor gives perfect measurements, and these inaccuracies manifest themselves as noise in the obtained measurements;
- Even when the object of interest is in the sensor's field of view, the sensor may fail to detect it;
- Sensors only give partial information about the state of the object, and so variables such as object velocity need to be estimated over time;
- The relation between measurements and object state is non-linear, which can complicate the state estimation process.

978-1-4673-7676-1/16/$31.00

The need to establish a clear estimate of the situation of orbital objects around Earth in spite of these difficulties, and the limited pool of available sensors that can provide data to do so, motivates the development of robust tracking techniques to accomplish this goal. The most commonly sensors that are used for space situational awareness (SSA) are radar and telescopes [1], neither of which is able to fully observe the state of the objects of interest. Radar measures azimuth, elevation, range and range rate of change through the Doppler effect, while telescopes measure azimuth, elevation, and their rates of change using optical properties of their sensors. Due to the lack of information in either case, it is necessary to integrate measurements over time in order to recover estimates of the full sensor state. Optical sensors are particularly interesting in this context, as they can observe objects that are out of the acquisition range of radar systems and do not need to reflect energy off objects in order to observe them, and will be the focus of this article.

This article presents a state estimation method that addresses the previously mentioned issues in an orbital tracking scenario, using measurements obtained from an optical sensor in order to construct an initial estimate for the orbit of an object based on a single measurement, and then integrate subsequent measurements to refine the estimate of its state. Although the method presented here is meant to track a single object, it can potentially be embedded in multi-sensor multiple target tracking frameworks such as the one presented in [2].

The rest of the article is divided as follows. First, the framework of Bayesian state estimation is introduced, followed by a description of the implemented filter. After this, results are shown, and conclusions are presented.

2. BAYESIAN STATE ESTIMATION

Even though the instruments used to observe Earth-orbiting objects are highly sophisticated, as with any sensor, measurements obtained with them are prone to being corrupted by noise. Additionally, sensors such as astrometric radar and electro-optical sensors do not observe the full state of the target, and the unobserved parameters are only known to be somewhere within an admissible region. Due to this, it is advantageous to estimate statistically the *probability distribution* of the state of the object rather than only a point estimate, as this also gives a measure of the uncertainty of the parameters. Bayesian estimation is a particular type of statistical estimation which uses Bayes' rule to update

a probability distribution, called the 'prior', using known information about the process and measurement, into a new distribution called the 'posterior' [3]. The problem of estimation for objects in orbit deals with using measurements from a sensor that observes the surveyed object in order to deduce a set of features of interest, such as position and velocity, alongside the associated estimation uncertainties.

Tracking can be defined as the process by which measurements obtained from an object of interest are used to maintain an estimate of its state [4]. It is evident that this can be readily cast into the framework of Bayesian estimation, and indeed research in tracking was revolutionised when Kalman published his seminal work relating the concept of system state estimation and probability theory [5]. This problem has been widely studied and is crucial for such relevant problems as the exploration of space, robotics, finance, and many others. The appeal of state estimation lies on the fact that it naturally accounts for the inherent uncertainty in the obtained measurements and in the modelling of the observed process, and reflects this in the variance of the estimated probability distribution. Additionally, it gives a reliable way of using previously acquired information to make predictions about the target state, even in situations where measurements are not available, and to infer information about variables that are not directly observed by the sensor.

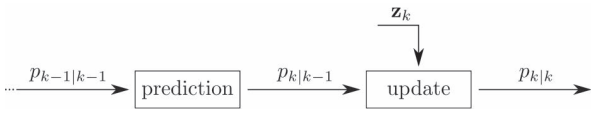

Figure 1. Data flow of a Bayesian filter.

Recursive Bayesian estimation, or Bayesian filtering, is a framework which attempts to track the state of a time-varying system in a statistically optimal way [3]. It does so by using the dynamic model of the system to perform a prediction step, and then using the likelihood function of received measurements conditioned on the state to perform an update step. The dynamic model is integrated into the prior through the Chapman-Kolmogorov equation, while the likelihood function adjusts it when measurements are received using Bayes' rule. This can be expressed as follows:

$$p_{k|k-1}(\mathbf{x}) = \int f(\mathbf{x}|\mathbf{x}')p_{k-1|k-1}(\mathbf{x}')\,\mathrm{d}\mathbf{x}' \tag{1}$$

$$p_{k|k}(\mathbf{x}) = \frac{g_k(\mathbf{z}_k|\mathbf{x})p_{k|k-1}(\mathbf{x})}{\int g_k(\mathbf{z}_k|\mathbf{x}')p_{k|k-1}(\mathbf{x}')\,\mathrm{d}\mathbf{x}'}, \tag{2}$$

where the following definitions are used:

$p_{k\|k-1}(\mathbf{x})$	predicted density up to time k,
$f(\mathbf{x}\|\mathbf{x}')$	probability of the target having state $\mathbf{x}$ given previous state $\mathbf{x}'$,
$p_{k\|k}(\mathbf{x})$	updated density up to time k, and
$g_k(\mathbf{z}_k\|\mathbf{x})$	likelihood of observing measurement $\mathbf{z}_k$ conditioned on state $\mathbf{x}$.

This generic filter is called the Bayes Filter. The general data flow for filters of this class can be seen in Fig. 1. Tractable implementations of the Bayes filter require choosing appropriate forms for the estimated probability distributions in order to be able to compute the predicted and updated probability distributions.

In a spatial tracking scenario, where it is attempted to recover the full state of an earth-orbiting object based on measurements from a sensor, the following steps must be carried out:

- Initialise the track using an initial measurement from the sensor (*initial orbit determination*),
- Predict the state of the object based on the motion model (*orbit propagation*),
- Correct this prediction using subsequent measurements given by the sensor, and
- Extract the state estimate from the resulting probability distribution.

The state itself is usually the position and velocity of the object of interest (e.g. a satellite, a piece of debris, or an asteroid) at each time step, while the type of measurements that will be considered in this article will be those coming from optical telescopes, which are assumed to yield azimuth, elevation and the rates of change of these angles. It is not possible to directly recover the range of the object and its rate of change from measurements of this type. This also implies that track initialisation needs to be carried out carefully, in order to accurately represent the uncertainty of the unobserved parameters. The proposed filter will be described in the next section.

3. FILTER DESCRIPTION

As it was previously mentioned, the Bayesian paradigm is a good fit for the problem of state estimation for Earth-orbiting objects. Designing a single-target filter following this framework involves coming up with solutions to the problems of *a*) track initialisation, *b*) time prediction, *c*) data update, and *d*) state extraction. The state of interest at time step k, denoted $\mathbf{x}_k$, will be the position and velocity of the Earth-orbiting object in the Earth-centred inertial (ECI) frame, i.e., $\mathbf{x}_k = [x_k, y_k, z_k, \dot{x}_k, \dot{y}_k, \dot{z}_k]'$, where prime denotes transposition. The measurements used for the data update come from a telescope, consisting of azimuth, elevation and their rates of change, in a frame of reference with origin in the sensor location, and will be denoted $\mathbf{z}_k = [\theta_k, \varphi_k, \dot{\theta}_k, \dot{\varphi}_k]'$.

Due to the non-linearities involved in track initialisation, state prediction and update, the particle filtering framework was used to construct the filter. Particle filtering is an approach which permits a high degree of flexibility in the design of priors, transition kernels and likelihood functions [6]. This is particularly useful in this case, due to the non-linear transformations between the different parameterisations of the state space that are used – although the prediction step is most naturally carried out in Cartesian space, the use of a full spherical frame is more convenient for track initialisation and update.

Mapping between spaces

The steps that need to be carried out to track objects in orbit using measurements from a ground-based telescope pose several challenges. Although some of the operations can be carried out linearly in the object state space, the non-linearities involved in the data update using this space can introduce error into the estimation process. To deal with this, the proposed filter changes between the object's state space $\mathbb{X}$ and the sensor's extended state space $\mathbb{S}^*$. If $\mathbf{x}_k = [x_k, y_k, z_k, \dot{x}_k, \dot{y}_k, \dot{z}_k]' \in \mathbb{X}$, its

equivalent vector in the sensor's state space is given by $\hat{\mathbf{z}}_k = T(\mathbf{x}_k, t_\mathrm{s}, W_\mathrm{s}) = [r_k, \theta_k, \varphi_k, \dot{r}_k, \dot{\theta}_k, \dot{\varphi}_k]'$, which can be computed as follows:

$$
\begin{aligned}
r_k &= \sqrt{\tilde{x}_k^2 + \tilde{y}_k^2 + \tilde{z}_k^2} \\
\theta_k &= \operatorname{atan}\frac{\tilde{y}_k}{\tilde{x}_k} \\
\varphi_k &= \operatorname{atan}\frac{\tilde{z}_k}{\sqrt{\tilde{x}_k^2 + \tilde{y}_k^2}} \\
\dot{r}_k &= \frac{\tilde{x}_k\dot{\tilde{x}}_k + \tilde{y}_k\dot{\tilde{y}}_k + \tilde{z}_k\dot{\tilde{z}}_k}{r_k} \\
\dot{\theta}_k &= \frac{\dot{\tilde{y}}_k\tilde{x}_k - \dot{\tilde{x}}_k\tilde{y}_k}{\tilde{x}_k^2 + \tilde{y}_k^2} \\
\dot{\varphi}_k &= \frac{\dot{\tilde{z}}_k(\tilde{x}_k^2 + \tilde{y}_k^2) - \tilde{z}_k(\tilde{x}_k\dot{\tilde{x}}_k + \tilde{y}_k\dot{\tilde{y}}_k)}{r^2\sqrt{\tilde{x}_k^2 + \tilde{y}_k^2}},
\end{aligned}
$$

where $\tilde{\mathbf{x}}_k = [\tilde{x}_k, \tilde{y}_k, \tilde{z}_k, \dot{\tilde{x}}_k, \dot{\tilde{y}}_k, \dot{\tilde{z}}_k]' = W_\mathrm{s}(\mathbf{x}_k - t_\mathrm{s})$, with t_s and W_s respectively the translation vector and rotation matrix from the geocentric reference frame to the sensor Cartesian reference frame. Rotating and translating the measurement is necessary as if the sensor is stationary on the surface of the Earth, it will capture measurements from different positions and orientations as the Earth rotates through time. Note that the transformation T is a bijection and thus it is always possible to map back to $\mathbb{X}$ by applying its unique inverse.

The advantage of using this parameterisation is that the mapping from the extended sensor state space $\mathbb{S}^*$ to the measurement space $\mathbb{S}$ is linear, which is advantageous for the filter update. Indeed, it is straightforward to obtain an optical measurement $\mathbf{z}_k = [\theta_k, \varphi_k, \dot{\theta}_k, \dot{\varphi}_k]'$ from $\hat{\mathbf{z}}_k \in \mathbb{S}^*$:

$$
\mathbf{z}_k = H\hat{\mathbf{z}}_k,
$$

with

$$
H = \begin{bmatrix} 0 & 1 & 0 & 0 & 0 & 0 \\ 0 & 0 & 1 & 0 & 0 & 0 \\ 0 & 0 & 0 & 0 & 1 & 0 \\ 0 & 0 & 0 & 0 & 0 & 1 \end{bmatrix}.
$$

Track initialisation

The challenge in initialising a track from a telescope measurement is that, if no additional information is known, it is not possible to exactly determine the range and range rate of the observed object in the initial time step. However, the couple $(r_0, \dot{r}_0)$ can be bounded using internal energy constraints, as proposed in [7, 8]. As only objects in closed orbits will be considered for this filter, the internal energy can be considered to be non-positive, that is,

$$
E = \frac{1}{2}|\dot{\mathbf{r}}|^2 - \frac{\mu}{|\mathbf{r}|} \leq 0, \tag{3}
$$

where μ is the product of the mass of the Earth and the gravitational constant, and $\mathbf{r}$ is the geocentric inertial position vector of the object of interest. The vectors $\mathbf{r}$ and $\dot{\mathbf{r}}$ can be expressed as follows:

$$
\begin{aligned}
\mathbf{r} &= \mathbf{r}_\mathrm{s} + \mathbf{r}\boldsymbol{\rho}_\mathrm{r} \\
\dot{\mathbf{r}} &= \dot{\mathbf{r}}_\mathrm{s} + \dot{r}\boldsymbol{\rho}_\mathrm{r} + r\dot{\theta}\boldsymbol{\rho}_\theta + r\dot{\varphi}\boldsymbol{\rho}_\varphi,
\end{aligned}
$$

where $\mathbf{r}_\mathrm{s}$ is the geocentric inertial position vector of the sensor, and

$$
\begin{aligned}
\boldsymbol{\rho}_\mathrm{r} &= [\cos\theta\cos\varphi, \sin\theta\sin\varphi, \sin\varphi]', \\
\boldsymbol{\rho}_\theta &= [-\sin\theta\cos\varphi, \cos\theta\cos\varphi, 0]', \text{ and} \\
\boldsymbol{\rho}_\varphi &= [-\cos\theta\sin\varphi, -\sin\theta\sin\varphi, \cos\varphi]'.
\end{aligned}
$$

Following the approach laid out in [7], the energy constraint (3) can be reformulated with this representation as follows:

$$
2E = \dot{r}^2 + w_1\dot{r} + T(r) - 2\frac{\mu}{\sqrt{S(r)}} < 0, \tag{4}
$$

where

$$
\begin{aligned}
S(r) &= r^2 + w_5 r + w_0, \\
T(r) &= w_2 r^2 + w_3 r + w_4, \\
w_0 &= \|\mathbf{r}_\mathrm{s}\|^\mathbf{2}, \\
w_1 &= 2\langle\dot{\mathbf{r}}_\mathrm{s}, \boldsymbol{\rho}_\mathrm{r}\rangle, \\
w_2 &= \dot{\theta}^2\cos^2\varphi + \dot{\varphi}^2, \\
w_3 &= 2\langle\mathbf{r}_\mathrm{s}, \dot{\theta}\boldsymbol{\rho}_\theta + \dot{\varphi}\boldsymbol{\rho}_\varphi\rangle, \\
w_4 &= \|\dot{\mathbf{r}}\|^2, \text{ and} \\
w_5 &= 2\langle\mathbf{r}_\mathrm{s}, \boldsymbol{\rho}_\mathrm{r}\rangle.
\end{aligned}
$$

From here, a rejection sampling approach is used to draw samples from a uniform distribution over the admissible region. To do this, a range value is randomly sampled from a region of interest, defined to be between 1.5 and 20 times the radius of the earth. Having chosen this value, the boundaries of inequality (4) are determined to find the admissible values for $\dot{r}$:

$$
\dot{r} \in (-w_1/2 - \zeta, -w_1/2 + \zeta) \tag{5}
$$

$$
\zeta = \frac{1}{2}\sqrt{w_1^2 - 4(T(r) - 2\mu/\sqrt{S(r)})} \tag{6}
$$

If ζ is complex, the chosen value for r is discarded and another value is sampled, until a real solution is found. When it is, a value for the range rate is sampled from the admissible values determined by the inequality to give an admissible $(r, \dot{r})$ couple. To add diversity to the remaining four parameters, these are sampled from a Gaussian distribution centred on the observed parameters themselves, with covariance matrix reflecting the uncertainty on the measured quantities. This process is repeated until the desired amount of samples has been found. This process is summarised in Algorithm 1.

Time Prediction

Time prediction is the operation through which the probability distribution of the tracked object is changed to reflect its dynamics after an amount of time passes. The transition matrix for the object can be obtained using Shepperd's approach [9] based on Goodyear's general solution for the two-body problem [10]. Since a Particle filter approach is being followed, computing the predicted distribution is as simple as using the transition matrix to predict the state for each particle in the prior distribution, and adding a measure of noise which accounts for the increased uncertainty in the absence of an observation. The weights in this case are unchanged. This process is summarised in Algorithm 2

Algorithm 1: Track initialisation algorithm

Data:
- Measurement $z = [\theta, \varphi, \dot{\theta}, \dot{\varphi}]$
- Range limits $r_{\min}, r_{\max}$
- Covariance for observed parameters R

Result: Initialised particle distribution $\{x_0^{(i)}, w_0^{(i)}\}_{i=1}^N$
for $i = 1 \dots N$ **do**
  `solution_found` $\leftarrow$ `false`
  while *not solution_found* **do**
    Sample $r^{(i)} \sim \mathcal{U}(\nabla_{\min}, \nabla_{\max})$
    Evaluate $w_0, w_1, w_2, w_3, w_4, w_5, T(r), S(r)$
    Evaluate ζ from (6)
    if ζ *is real* **then**
      `solution_found` $\leftarrow$ `true`
end

end
  Sample $\dot{r}^{(i)} \sim \mathcal{U}(-w_1/2 - \zeta, -w_1/2 + \zeta)$
  Sample $[\theta^{(i)}, \varphi^{(i)}, \dot{\theta}^{(i)}, \dot{\varphi}^{(i)}]' \sim \mathcal{N}(\cdot; z, R)$
  $x_0^{(i)} \leftarrow T^{-1}([r^{(i)}, \theta^{(i)}, \varphi^{(i)}, \dot{r}^{(i)}, \dot{\theta}^{(i)}, \dot{\varphi}^{(i)}]')$
  $w_0^{(i)} \leftarrow 1/N$
end

Algorithm 2: Prediction algorithm

Data:
- Particle distribution $\{x_{k-1}^{(i)}, w_{k-1}^{(i)}\}_{i=1}^N$ at time step $k-1$
- Covariance matrix of the process noise Q_k
- Elapsed amount of time Δ_t
- Translation and rotation to sensor Cartesian frame $t_{\mathrm{s}}, W_{\mathrm{s}}$

Result: Predicted particle distribution $\{x_{k|k-1}^{(i)}, w_{k|k-1}^{(i)}\}_{i=1}^N$
for $i = 1 \dots N$ **do**
  Sample $\epsilon_i \sim N(0, Q_k)$
  $\Phi \leftarrow$ `Shepperd_matrix` $(x_{k-1}^{(i)}, \Delta_t)$
  $x_{k|k-1}^{(i)} \leftarrow \Phi x_{k-1}^{(i)} + \epsilon_i$
  $w_{k|k-1}^{(i)} \leftarrow w_k^{(i-1)}$
end

Data Update

Although the state space $\mathbb{X}$ is convenient to perform state prediction, constructing a measurement likelihood function in this space is complicated due to the non-linearity of the mapping between both spaces (See Section 3). As it was seen before, however, the transformation between the extended sensor state space $\mathbb{S}^*$ and the measurement space $\mathbb{S}$ is linear, which simplifies estimation. Since both spaces are useful, a hybrid approach is proposed which makes use of them both. If no measurements are received, the prediction step is carried out as described in Section 3. However, if a measurement is received, the linearity of the measurement likelihood is exploited to obtain the updated distribution. The proposed algorithm first maps the particles to the augmented sensor space $\mathbb{S}^*$ and approximates the resulting particle distribution as a Gaussian distribution. This distribution is updated using linear Kalman update in this space, and the resulting Gaussian distribution, which will be denoted $\pi(x|x_{0:t}, z_{0:t})$, is used to sample the new point cloud. Note that although particles are used to represent this distribution, these are unweighted as opposed to a traditional bootstrap filter. This approach has been successfully used in applications such as multiple-object tracking using stereo cameras [11], and multiple object tracking for SSA using radar [2]. This process is illustrated in Algorithm 3.

Algorithm 3: Update algorithm

Data:
- Predicted particle distribution $\{x_{k|k-1}^{(i)}\}_{i=1}^N$ at time step k
- Measurement $z = [\theta, \varphi, \dot{\theta}, \dot{\varphi}]$
- Covariance matrix of the noise R_k

Result: Updated particle distribution $\{x_k^{(i)}\}_{i=1}^N$
for $i = 1 \dots N$ **do**
  $\hat{y}_i^- \leftarrow T(\mathbf{x}_{k|k-1}^{(i)}, t_{\mathrm{s}}, R_{\mathrm{s}})$
end
$\mu_k^- \leftarrow$ `mean` $(\{y_i^-\}_{i=1}^N)$
$\Sigma_k^- \leftarrow$ `covariance` $(\{y_i^-\}_{i=1}^N)$
Compute Kalman Filter updated mean and covariance
$\xi \leftarrow z - H\mu_k^-$
$S \leftarrow H\Sigma_k^- H' + R_k$
$K \leftarrow \Sigma_k^- H' S^{-1}$
$\mu_k \leftarrow \mu_k^- + K\xi$
$\Sigma_k \leftarrow (I - KH)\Sigma_k^-$
for $i = 1 \dots N$ **do**
  Sample $y_i \sim N(\mu_k, \Sigma_k)$
  $x_k^{(i)} \leftarrow T^{-1}(y_i, t_{\mathrm{s}}, R_{\mathrm{s}}))$
end

State Extraction

Due to the nature of orbital mechanics, the spread of particles after prediction will tend to lay along the same orbit and thus take a banana-shaped distribution. Taking the Expected A Posteriori (EAP) estimate from the distribution in the Cartesian space $\mathbb{X}$, then, will introduce bias in the estimated orbit. To solve this, the proposed method maps the distribution into the augmented sensor frame $\mathbb{S}^*$, computes the EAP in this space, and then maps this value back into $\mathbb{X}$ as the filter output. The situation is illustrated in Figure 2, where it can be seen that the filter estimate agrees more with the estimated orbit as predicted by the orbital dynamics. The method is described in Algorithm 4.

Algorithm 4: State estimate extraction process

Data:
- Particle distribution $\{x_k^{(i)}, w_k^{(i)}\}_{i=1}^N$ at time step k

Result: Estimated state $\hat{x}_k$
for $i = 1 \dots N$ **do**
  $\hat{y}_i \leftarrow T(\mathbf{x}_k^{(i)}, t_{\mathrm{s}}, R_{\mathrm{s}})$
end
$\mu_k \leftarrow$ `mean` $(\{y_i\}_{i=1}^N)$
$\hat{x}_k \leftarrow T^{-1}(\mu_k, t_{\mathrm{s}}, R_{\mathrm{s}}))$

4. RESULTS

To demonstrate the performance of the filter, a simulated orbital scenario was generated with two different objects in orbit. The orbits were created from the initial orbital elements utilizing Runge-Kutta $7/8$ numerical integration, taking into account the Earth's gravitational field up to order and degree

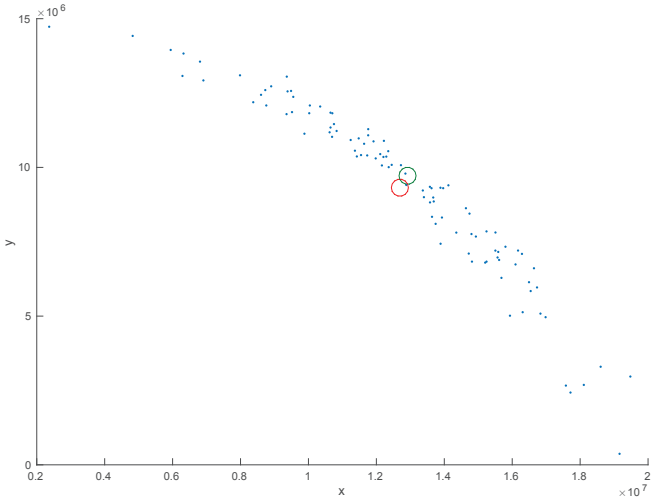

Figure 2. EAP of the Cartesian distribution (red circle) compared to the proposed state estimate (green circle).

T.	a (km)	e	i	Ω	ω	ν
1	26352.5	0.6	11.3°	69.0°	351.0°	80.0°
2	42164.0	0.012	10.0°	61.0°	349.0°	82.0°

Table 1. Target index, semi-major axis (a), eccentricity (e), inclination (i), right ascension of the ascending node (Ω), argument of perigee (ω) and true anomaly (ν).

12, third body perturbations of the Sun and Moon as well as direct radiation pressure. More details about the propagation models used for this simulation can be found in [12]. The shape of the objects was assumed to be spherical, and the area to mass ratio was simulated as 0.02 for both objects. The remaining target characteristics are listed in Table 1, and an illustration of the scenario can be seen in Figure 3.

The simulated sensor is a ground-based telescope with a field of view of $8° \times 8°$, at a latitude of $20°$. A standard deviation of a quarter of an arcsecond was assumed for each of the four observed quantities - azimuth, elevation, and their rates of change. Measurements were triggered each time the objects passed the sensor's field of view, at a rate of one measurement every twenty seconds. The orientation of the telescope was different for both simulations, in order to obtain meaningful information about each orbit. The simulated trajectories and the field of the sensor can be seen in Fig. 3. The filter was executed with 2000 particles in every case.

The main challenges present in the simulated scenarios are the following:

1. Tracks must be initialized from an initial measurement, which does not contain full information on its state, and refined through subsequent observations,
2. When an object exits the narrow field of view of the sensor, the uncertainty in the estimation grows continually until it is observed again, and
3. The uncertainty on the estimated distribution must be reduced once measurements are available again.

For target one, the main issue is that measurements are acquired only during two periods in the simulation, although the length of time is sufficient to correctly establish the orbit of the object. In Fig. 4, the results of the estimation for a sample run of the filter can be seen. The periods where the target is observed are shown in red, where initialisation and correction are performed. The dotted black lines show the estimated trajectory when only prediction is performed. Visually, the estimated orbit agrees well with the ground truth. In terms of quantitative performance metrics, the estimation is evaluated using the root mean squared error (RMSE) to analyse the filter's accuracy, and the Mahalanobis distance to determine if the estimated distribution accurately reflects the uncertainty in the estimation, which can be seen in Fig. 5. To give a sense of scale to the Mahalanobis distance, for a 6-dimensional multivariate Gaussian random variable, 95% of the probability density is contained within a Mahalanobis distance of 12.5916. These metrics were obtained by averaging over 50 Monte Carlo runs.

Target two presents different challenges. As it can be seen in Fig. 6, the target is only observed for very brief amounts of time, after which the information must be propagated for a long amount of time before being able to observe it again. In spite of this, the filter manages to initialise the orbit reasonably well, and correct its estimate as new measurements arrive. As before, 50 Monte Carlo runs were executed, and the average performance metrics can be seen in Fig. 7. Even in spite of the very short time spans where the target is seen, the estimation error is kept reasonably low, and as before the Mahalanobis distance shows that the estimated distribution accurately represents the uncertainty with respect to the true trajectory.

Comparison to Other Approaches

The typical filters that are used to track single targets in the presence of non-linear motion and measurement models are the extended Kalman filter (EKF), and the particle filter. The EKF is based on a linearisation of these models, and is based on the assumption that the prior distributions are reasonably close to a Gaussian. As it was seen previously, however, the initial orbit determination algorithm which is used to initialise these filters is drawn from an uniform distribution in a region with non-linear bounds in the extended sensor space, which should not be expected to be Gaussian. Even if after a series of observations the estimated posterior is localised enough that it can be considered to be Gaussian in Cartesian space, the prediction process will propagate the distribution along an orbit, creating a banana-shaped distribution which cannot be considered Gaussian in this space. To show this numerically, the BHEP Gaussianity test [13] was applied to the particle clouds produced by the filter for target 1, and the resulting p-value was averaged over 200 Monte Carlo runs, which can be seen in Figure 8. The test compares the empirical characteristic function of the sampled distribution against that of a Gaussian distribution, the null hypothesis being that the samples come indeed from a distribution of this type. If the p-value drops below a chosen significance level, the assumption of Gaussianity can be rejected. As it can be seen in the figure, the test rejects Gaussianity for a period after the particle cloud is initialised. After this, it can be considered Gaussian as it becomes more localised. After observations cease to be used to correct the distribution, the Gaussianity of the distribution degrades until it can no longer be considered Gaussian. Due to this reason, it can be concluded that the EKF is unfit to estimate this type of distributions.

In cases where the shape of the filtered distribution is unknown or cannot be analytically described, the standard approach is the bootstrap particle filter [14]. For comparison, this filter was used to estimate the satellite trajectories for the same data used in these experiments, using 5000 particles.

As it was expected, however, the filter diverged in every case. This is due to a combination of the highly non-linear motion and measurement models and the high dimensionality of the data.

5. CONCLUSIONS

In this article, an algorithm was presented which uses telescope measurements to track orbital objects in space, by exploiting the fact that the measurement model is linear in the sensor's extended measurement space. The major advantages of this method are that the resulting estimation is probabilistic, and so gives information on the uncertainty of the estimate; that track initialisation is also done probabilistically and allows for information to be sequentially integrated into the distribution in order to refine it, and that it is easily embeddable in more sophisticated multiple target tracking solutions. To evaluate the performance of the method, it was applied to two simulated objects in orbit, showing good performance even when measurements were scarce due to the limited field of view of the object.

ACKNOWLEDGMENTS

This work was supported by the Engineering and Physical Sciences Research Council (EPSRC) Grant number EP/K014277/1 and the MOD University Defence Research Collaboration in Signal Processing.

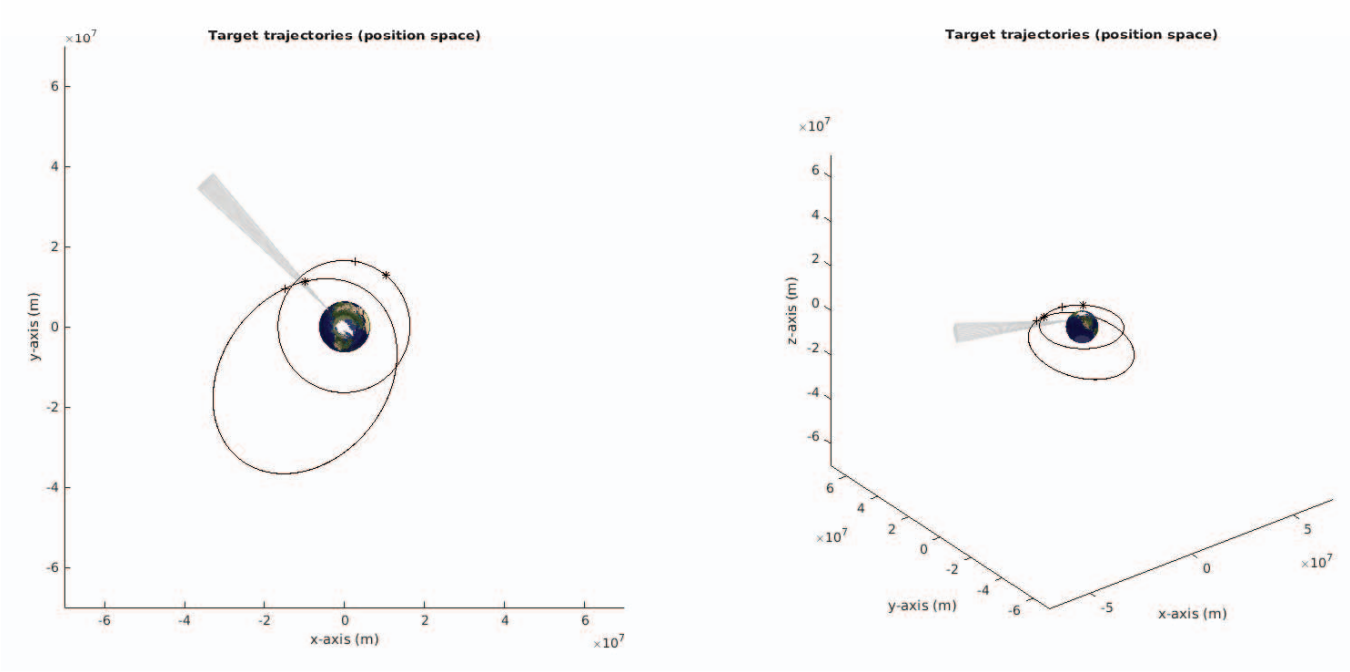

Figure 3. Illustration of the simulated scenario, including the two targets orbiting Earth and the sensor's field of view. The wider orbit with higher eccentricity is target 1, and the smaller one is target 2.

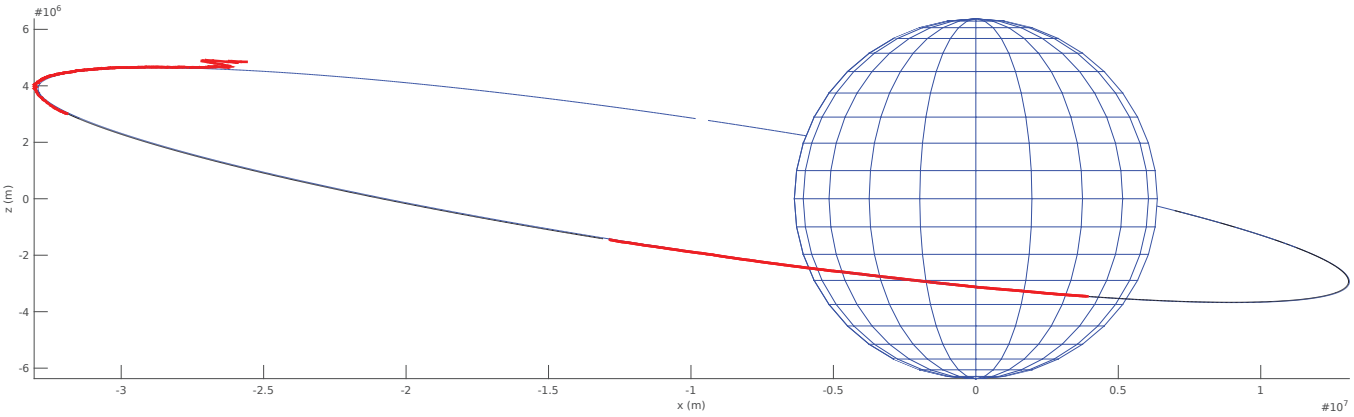

Figure 4. Simulated eccentric orbit (target 1) and estimation results. The blue line shows the actual trajectory, the thick red lines the estimated trajectory in periods where the target is observed and dotted black when not. The blue sphere represents the Earth.

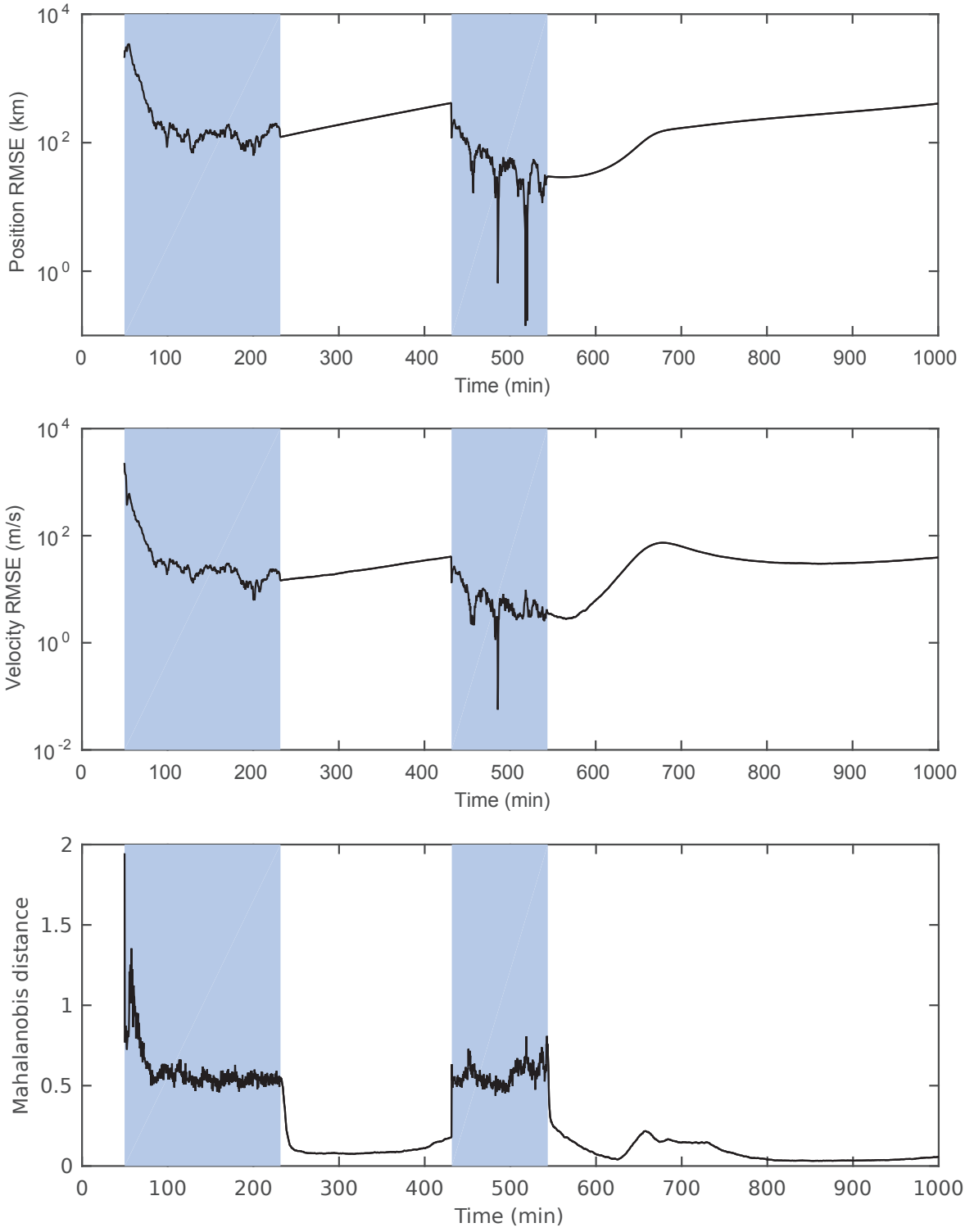

Figure 5. Performance metrics for the estimation of the first orbit. Above, RMSE for position and velocity (logarithmic scale), followed by the Mahalanobis distance between the estimated distribution and the ground truth trajectory. The lengths of time when the target is observed are shaded in blue.

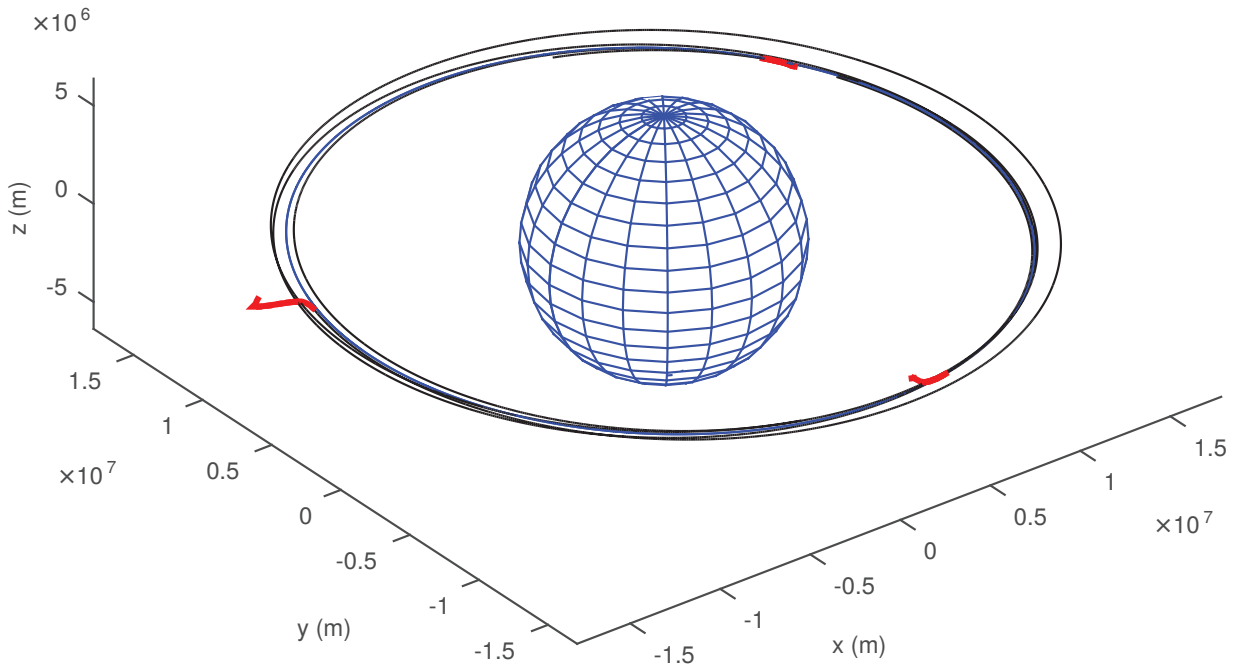

Figure 6. Simulated low earth orbit (target 2) and estimation results. The blue line shows the actual trajectory, the thick red lines the estimated trajectory in periods where the target is observed and dotted black when not. The blue sphere represents the Earth.

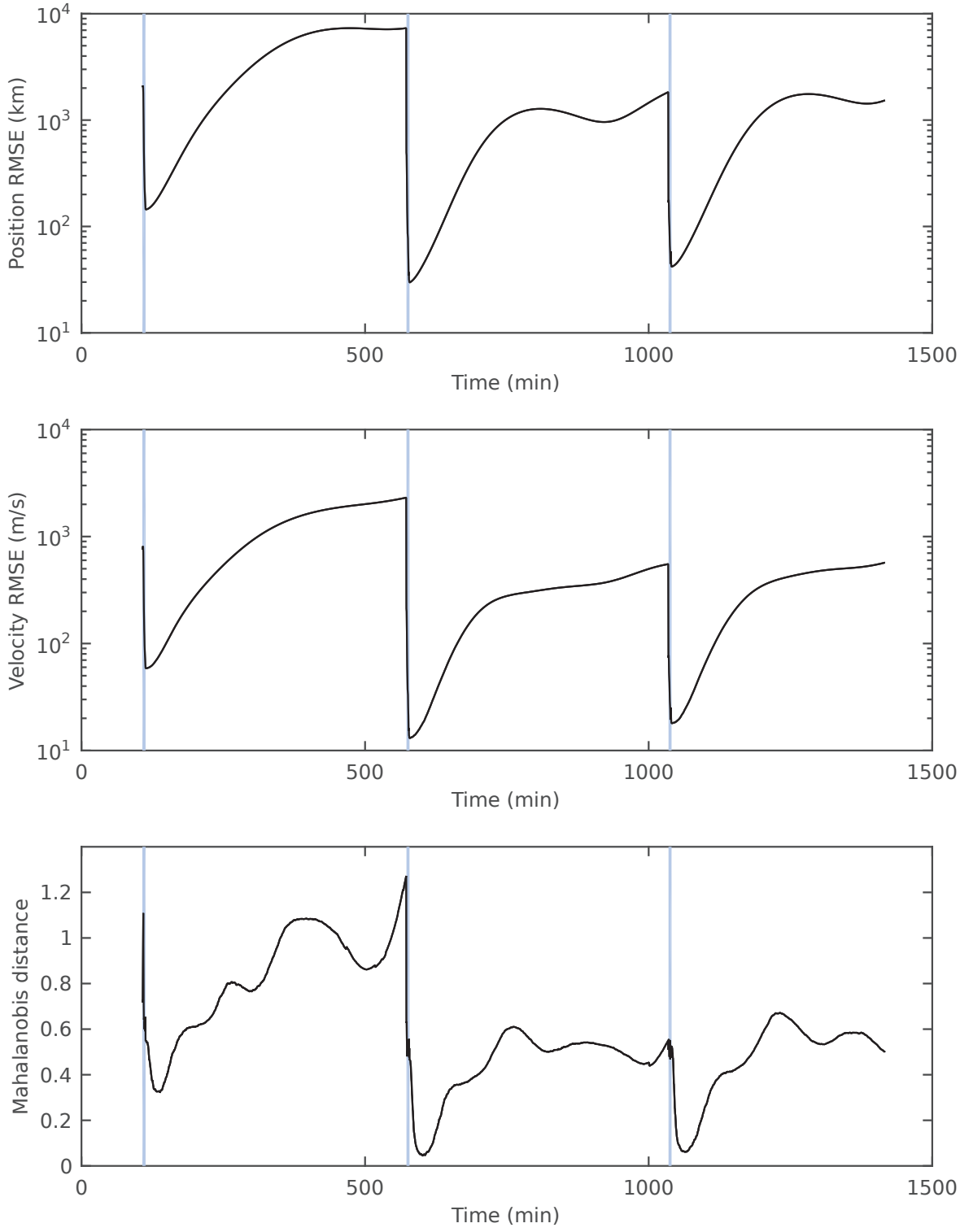

Figure 7. Performance metrics for the estimation of the second orbit. Above, RMSE for position and velocity (logarithmic scale), followed by the Mahalanobis distance between the estimated distribution and the ground truth trajectory. The lengths of time when the target is observed are shaded in blue. The values shown are the average over 50 Monte Carlo runs.

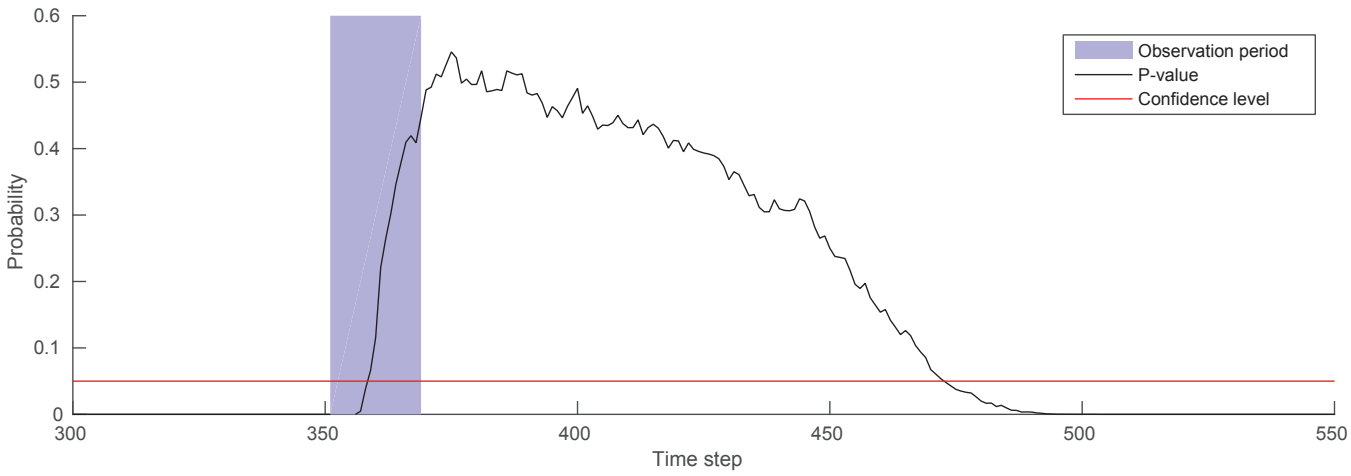

Figure 8. Averaged p-values of the BHEP test for the estimated probability distribution. When the p-value is below the confidence level, the hypothesis of Gaussianity is rejected.

REFERENCES

[1] A. Rossi, "The earth orbiting space debris," *Serbian Astronomical Journal*, vol. 170, pp. 1–12, 2005.

[2] E. Delande, C. Frueh, J. Houssineau, and D. Clark, "Multi-object filtering for space situational awareness," in *Proceedings of the 25th AAS/AIAA Space Flight Mechanics Meeting*, Williamsburg, VA, 2014.

[3] S. Särkkä, *Bayesian filtering and smoothing*. Cambridge University Press, 2013.

[4] Y. Bar-Shalom and T. E. Fortmann, *Tracking and Data Association*. San Diego, CA, USA: Academic Press Professional, Inc., 1987.

[5] R. E. Kalman, "A new approach to linear filtering and prediction problems," *Journal of Fluids Engineering*, vol. 82, no. 1, pp. 35–45, 1960.

[6] A. Doucet, N. de Freitas, and N. Gordon, Eds., *Sequential Monte Carlo Methods in Practice*. Springer-Verlag, 2001, vol. 1.

[7] G. Tommei, A. Milani, and A. Rossi, "Orbit determination of space debris: admissible regions," *Celestial Mechanics and Dynamical Astronomy*, vol. 97, no. 4, pp. 289–304, 2007.

[8] D. Farnocchia, G. Tommei, A. Milani, and A. Rossi, "Innovative methods of correlation and orbit determination for space debris," *Celestial Mechanics and Dynamical Astronomy*, vol. 107, no. 1-2, pp. 169–185, 2010.

[9] S. W. Shepperd, "Universal Keplerian state transition matrix," *Celestial Mechanics*, vol. 35, pp. 129 – 144, 1985.

[10] W. H. Goodyear, "Completely general closed-form solution for coordinates and partial derivative of the two-body problem," *Astronomical Journal*, vol. 70, no. 3, pp. 189 – 192, 1965.

[11] J. Houssineau, D. Clark, S. Ivekovic, C. S. Lee, and J. Franco, "A unified approach for multi-object triangulation, tracking and camera calibration," *IEEE Transactions in Signal Processing*, 2016 (forthcoming).

[12] C. Früh, T. M. Kelecy, and M. K. Jah, "Coupled orbit-attitude dynamics of high area-to-mass ratio (hamr) objects: influence of solar radiation pressure, earths shadow and the visibility in light curves," *Celestial Mechanics and Dynamical Astronomy*, vol. 117, no. 4, pp. 385–404, 2013.

[13] N. Henze and B. Zirkler, "A class of invariant consistent tests for multivariate normality," *Communications in Statistics-Theory and Methods*, vol. 19, no. 10, pp. 3595–3617, 1990.

[14] N. J. Gordon, D. J. Salmond, and A. F. Smith, "Novel approach to nonlinear/non-gaussian bayesian state estimation," in *IEE Proceedings F (Radar and Signal Processing)*, vol. 140, no. 2. IET, 1993, pp. 107–113.

BIOGRAPHY

Jose Franco *received a B.Sc. degree in mathematical engineering from EAFIT University in 2010 and a M.Sc. in computer vision and robotics jointly from the University of Burgundy, the University of Girona and Heriot-Watt University in 2013. He is currently a doctoral student in Heriot Watt University under the supervision of Dr Daniel Clark, where he studies multiple object estimation techniques for a variety of applications.*

Emmanuel D. Delande *received an Eng. degree from the Ecole Centrale de Lille, Lille, and a M.Sc. degree in automatic control and signal processing from the University of Science & Technology, Lille, both in 2008. He was awarded his Ph.D. in 2012 from the Ecole Centrale de Lille. He is a research associate at Heriot-Watt University in Edinburgh. His research interests are in the design and the implementation of multi-object filtering solutions for multiple target tracking and sensor management problems.*

Carolin Frueh *was awarded a PhD in Physics with Specialization in Astronomy from the University of Bern, Switzerland, under supervision of Prof. Dr. Thomas Schildknecht in 2011. After this, she took a National Research Council post-doctoral position with the Air Force Research Laboratory, Kirtland under supervision of Dr Moriba Jah until 2013, followed by a position as a Research Scientist with Texas A&M University with Prof. Dr. Terry Alfriend until 2014. She is currently an assistant professor in Purdue University.*

Jérémie Houssineau *received an Eng. degree in mathematical and mechanical modelling from MATMECA, Bordeaux, and a M.Sc. degree in mathematical modelling and statistics from the University of Bordeaux, both in 2009. From 2009 to 2011, he was a Research Engineer with DCNS, Toulon, and then with INRIA Bordeaux. He received his Ph.D. degree in statistical signal processing from Heriot-Watt University, Edinburgh, in 2015. His research interests include applied probability, point process theory and multi-object estimation.*

Daniel E. Clark *is an Associate Professor in the School of Engineering and Physical Sciences at Heriot-Watt University. His research interests are in the development of the theory and applications of multi-object estimation algorithms for sensor fusion problems. He has led a range of projects spanning theoretical algorithm development to practical deployment. He was awarded his Ph.D. in 2006 from Heriot-Watt University.*